CHINESE OPTICS LETTERS

Vol. 21, No. 2 | February 2023

Widely tunable 2 μm optical vortex from a Tm:YAP laser

Jingjing Zhou (周晶晶)[1], Changsheng Zheng (郑昌盛)[1], Bin Chen (陈 彬)[2,3], Ning Zhang (张 宁)[2,3], Qinggang Gao (高庆港)[2,3], Hangqi Yuan (袁航琪)[1], Daiwen Jia (贾代文)[1], Zhanxin Wang (王占新)[1*], Shande Liu (刘善德)[2], Yuping Zhang (张玉萍)[2], Huiyun Zhang (张会云)[2], and Yongguang Zhao (赵永光)[1,3**]

[1] Jiangsu Key Laboratory of Advanced Laser Materials and Devices, Jiangsu Normal University, Xuzhou 221116, China

[2] College of Electronic and Information Engineering, Shandong University of Science and Technology, Qingdao 266590, China

[3] Jiangsu Collaborative Innovation Center of Advanced Laser Technology and Emerging Industry, Jiangsu Normal University, Xuzhou 221116, China

*Corresponding author: lqwang929@163.com

**Corresponding author: Yongguangzhao@yeah.net

Received June 22, 2022 | Accepted August 15, 2022 | Posted Online September 21, 2022

In this paper, we report on a wide wavelength tuning optical vortex carrying orbital angular momentum (OAM) of ±ℏ, from a thulium-doped yttrium aluminum perovskite (YAP) laser employing a birefringent filter. The OAM is experimentally found to be well maintained during the whole wavelength tuning process. The Laguerre–Gaussian ($LG_{0,+1}$) mode with a tuning range of 58 nm from 1934.8 to 1993.0 nm and $LG_{0,-1}$ mode with a range of 76 nm from 1920.4 to 1996.6 nm, are, respectively, obtained. This is, to the best of our knowledge, the first experimental implementation of wavelength tuning for a scalar vortex laser in the 2 μm spectral range, as well as the broadest tuning range ever reported from the vortex laser cavity. Such a vortex laser with robust structure and straightforward wavelength tuning capability will be an ideal light source for potential applications in the field of optical communication with one additional degree of freedom.

Keywords: wavelength tunable laser; 2 μm laser; orbital angular momentum.

DOI: 10.3788/COL202321.021405

1. Introduction

The optical vortex generally refers to the Laguerre–Gaussian (LG_{0l}) mode with a spiral phase term of $\exp(il\varphi)$ in its complex amplitude expressed in cylindrical coordinates, where l is the topological charge. In addition to the conventional spin angular momentum (SAM), the attractive property of the optical vortex is that it can carry a well-defined orbital angular momentum (OAM) of $l\hbar$ per photon[1]. Due to the existence of OAM, the optical vortex exhibits wide applications in fields such as optical communication to increase the transmission capacity[2], optical tweezers to manipulate the particles[3], and detection of a spinning object[4]. Up to now, various methods have been exploited for the production of optical vortices. Basically, they can be divided into two categories: intracavity mode selection and extra-cavity mode conversion. The implementation of extra-cavity mode conversion is mainly based on transformation of other transverse laser modes into a vortex beam by using optical phase elements, like cylindrical lens[5], spiral phase plate[6], forking grating[7], and spatial light modulators[8]. Such technique has advantages of simple operation, enabling generation of different orders of vortex beams; however, the other side suffers from drawbacks of low power level and wavelength sensitivity due to the dependence on material properties such as the refractive index and laser damage threshold. Alternatively, the intracavity mode-selection technique, i.e., direct generation of vortex beams from a laser cavity, can overcome these drawbacks and enable the production of optical vortices with a high power level, high beam quality, and, in particular, the potential for wavelength tuning. One notable thing in such a laser cavity is the synchronous oscillation of the vortex beams with opposite handedness due to their same spatial intensity distribution along the gain media[9–12], which will result in a coherent superposition of these two beams to form a "petal-like" mode with zero total OAM. Fortunately, a few methods, such as intracavity nanoscale aluminum stripes[9], propagation symmetry broken in combination with Fresnel reflection loss[10], polarization states separation[11], and asymmetric resonator loss induced frequency degeneracy[12,13], have been exploited to control the handedness, thus making it possible for such vortex lasers for practical applications outside specialized laboratories.

Nowadays, generation and modulation of OAM in the laser cavities have been intensively studied with different techniques, such as spot-defect mirror[14], annular-shape beam pumping[15,16], and intracavity spiral phase plate[17]. However, wavelength tuning of vortex beams with well-maintained spatial amplitude and phase structure is scarcely reported from a laser cavity. To date, the reflective volume Bragg grating (VBG) has been theoretically and experimentally proved to be an effective wavelength selector for optical vortices with well-conserved OAM[18]. Most recently, a birefringent filter (BF) was experimentally used in a Yb:$CaGdAlO_4$ (Yb:CALGO) vortex laser and exhibited similar wavelength tuning ability for vortex beams[19]. Unfortunately, all of the previous reports have been focused on the near-infrared (IR) spectral region, and the wavelength tuning range was less than 50 nm limited by the gain spectrum of laser materials or cavity design[18,19]. So, wide tunability of the vortex laser, in particular, in the mid-IR region is desired from the viewpoint of their potential applications.

The thulium-doped yttrium aluminum perovskite (Tm:YAP) crystal has a high quantum efficiency for laser operation at 2 μm due to the existence of a self-quenching mechanism between the $^3H_4$ and $^3F_4$ energy levels. Laser emission from the $^3F_4 \rightarrow {}^3H_6$ transition has been observed in the spectral range of 1.86–2.03 μm[20,21]. In addition, the absorption band related to a transition from the $^3H_6$ to $^3H_4$ level can be easily pumped by a high-power commercial AlGaAs laser diode (LD) at 795 nm. This makes it a perfect gain media for the wavelength tuning laser in the 2 μm spectral range. In this paper, we have experimentally demonstrated a broad wavelength tuning range of the vortex laser in the 2 μm spectral range from a Tm:YAP laser by employing a BF as the wavelength selector. The produced optical vortices with a broad wavelength tuning range will have potential applications in optical communication with a combination between wavelength-division multiplexing (WDM) and OAM mode-division multiplexing (OAM-MDM).

2. Cavity Design and Experimental Layout

Generation of a vortex laser in this work was realized by using an annular pumping technique, which is, in principle, based on a selection of the transverse mode in the cavity. The BF is a 2-mm-thick octagonal quartz plate (a uniaxial crystal with refractive index of $n_o = 1.5209$ and $n_e = 1.5291$ at 2 μm[22]) with its optical axis parallel to the surface that has been optically polished. Since the BF was placed in the cavity at a Brewster's angle[23,24], the oscillated laser in the cavity has specific linear polarization. The laser with the lowest threshold power will preferentially oscillate. According to the relationship $P_{th} \propto A_{eff}$[25], where P_{th} and A_{eff} represent threshold power and effective pump area, respectively, the mode that matches the smallest A_{eff} will be oscillated first. Figure 1(a) shows the calculated P_{th} of the three lowest order LG modes [transverse electromagnetic (TEM_{00}), $LG_{0,\pm1}$, and $LG_{0,\pm2}$] versus the cavity length L. Here, the reshaped pump beam has a near-field annular intensity profile with a 300 μm inner diameter and an outer diameter of 500 μm. Note that $LG_{0,+1}$ and $LG_{0,-1}$ (or $LG_{0,+2}$ and $LG_{0,-2}$) are a pair of degenerate modes thus exhibiting the same threshold pump power. To obtain a single transverse mode laser operation at the TEM_{00} or $LG_{0,\pm1}$ mode, the cavity length L should be in the range of 152–180 mm (region III) or 50–152 mm (II), respectively.

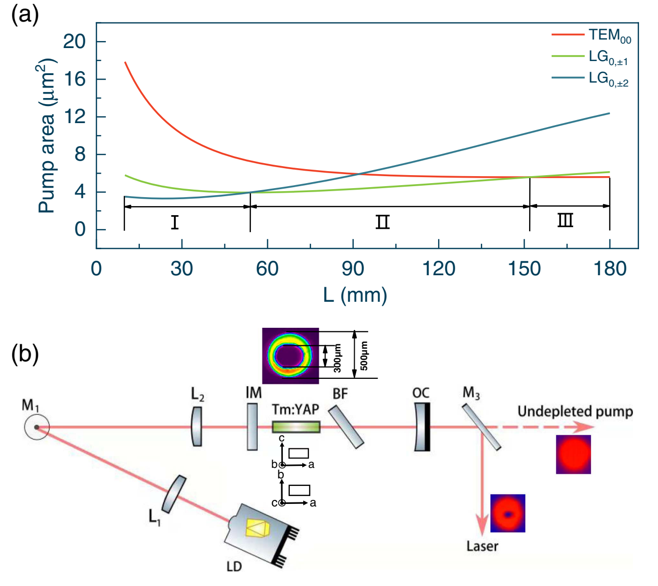

Fig. 1. (a) Calculated effective pumping areas versus cavity length for different LG modes with an annular pump. (b) Schematic of the 2 μm wavelength-tunable Tm:YAP vortex laser. LD, laser diode; L, lens; IM, input mirror; BF, birefringent filter; OC, output coupler.

Figure 1(b) shows the schematic of the wavelength tuning vortex laser. The pump source (LD) was a fiber (100 μm core diameter and 0.22 NA) coupled LD with a center wavelength of 793 nm. The pump light was at first collimated by a plano-convex lens (L_1) with a focal length of 25.4 mm, then was reflected by a hollow mirror (M_1, 2-mm central hole), and reshaped to an annular beam. Finally, the reshaped pump beam was focused into the center of the laser crystal by a lens (L_2) with $f = 150$ mm. The gain medium is an *a*-cut YAP crystal (orthorhombic, *Pnma* space group) doped with 3% (atomic fraction) thulium ion (Tm^{3+}). The crystal has the dimensions of 6 mm (*a*) × 4 mm (*b*) × 4 mm (*c*), and its two end faces were antireflective coated at 1900–2150 nm. To mitigate the thermal load, the crystal was wrapped with indium foil and tightly mounted in a copper holder which was water cooled to 15.0°C. The resonator was a standard hemispherical cavity including a plane input mirror (IM) and a plane-concave output coupler (OC) with radius of curvature of $R_{OC} = 200$ mm. In this work, the experimentally optimized transmission of the OC was 10%. Beam profiles and the corresponding self-interference patterns were recorded by using a mid-IR CCD camera (Xeva-1.7) together with a homemade Mach–Zehnder interferometer.

3. Results and Discussions

For comparison, we at first studied the tuning performance of the fundamental mode by adjusting the cavity to a length of $L = 160$ mm, i.e., in region III, as shown in Fig. 1(a). Without the BF, the laser was linearly polarized (extinction ratio of 28 dB) along the *b* axis due to the natural birefringence of the

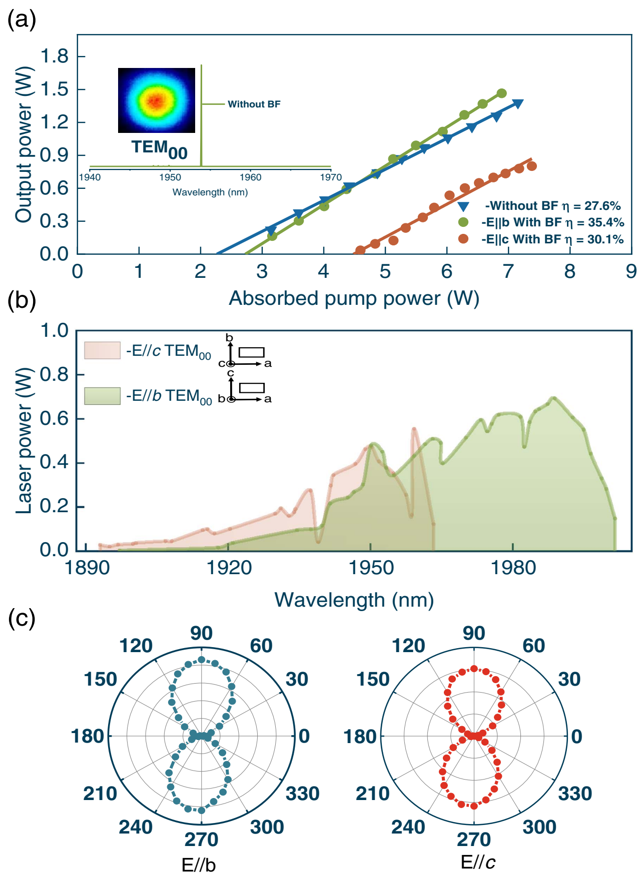

Fig. 2. (a) Laser slope efficiency, (b) wavelength tuning performance, and (c) the polarization measurement of the annular light pumped Tm:YAP laser with E‖*b* and E‖*c* polarization. Inset in (a): beam pattern and the corresponding optical spectrum of the Tm:YAP laser without BF.

crystal. As can be seen in Fig. 2(a), the laser slope efficiency was 27.6% with respect to the absorbed pump power, and the peak wavelength of the optical spectrum at the highest power was located at 1953.8 nm. Wavelength tuning was realized by inserting the BF in the cavity at a Brewster's angle. Since the BF mandated that the laser has horizontal polarization, wavelength tuning of the laser with polarization of E‖*b* or E‖*c* can be obtained just by rotating the laser crystal 90 deg along its *a* axis. For the E‖*b* laser, the laser slope efficiency was 35.4%. As shown in Fig. 2(b), the corresponding wavelength tuning range was 104 nm from 1897.1 to 2001.5 nm at an output power of 0.69 W. For the case of the E‖*c* laser, the threshold absorbed pump power increased to 4.6 W due to the smaller emission cross section of Tm:YAP crystal in this direction[26], and the laser slope efficiency was decreased to 30.1%. In this case, the tuning range was only 70 nm from 1893 to 1963.3 nm, because, in this case, a larger population inversion ratio was required for lasing, thus resulting in a narrower effective gain bandwidth. With a Glan-type polarizer, the polarization states of both laser beams were measured. Figure 2(c) shows the transmitted laser power as a function of rotation angle in polar coordinates, and the extinction ratio of E‖*b* and E‖*c* laser was measured to be 39.3 and 35.0 dB, respectively, higher than that without the BF.

Following the theoretical analysis, wavelength tuning of the optical vortices ($LG_{0,\pm1}$) was thereafter studied by shortening the laser cavity to a length of 110 mm, i.e., locating in region II, as shown in Fig. 1(a). To select the pure $LG_{0,+1}$ (or $LG_{0,-1}$) mode, i.e., handedness control, additional asymmetric loss that was introduced by slightly misaligning the laser cavity, is necessary to reduce the frequency difference of the intracavity eigen modes, thus forming an LG mode with well-defined handedness[12,13,27,28]. For the E‖*c* laser, which has a lower gain as in the case of the fundamental beam, the threshold absorbed pump power for the $LG_{0,+1}$ (or $LG_{0,-1}$) mode was 4.8 W. A slight change of the pump power or rotation of the BF will destroy the spatial structure of the optical vortex, leading to mode instability or mixing. We attributed this to the thermal lens effects at a high level of absorbed pump power; this was confirmed from the slightly improved stability by decreasing the temperature of the cooling system. Figure 3 shows the simulated beam radius in the crystal as a function of the absorbed pump power, i.e., different thermal lens effect[29]. For example, when the absorbed pump power of E‖*c* was 5.5 W, the calculated focal length of the thermal lens was about $f = 181$ mm, corresponding to a beam radius of 318 μm. This means the laser was operated at the edge of region III, as seen in Fig. 3, thus leading to an emission of a mixed mode, as shown by the inset. Therefore, it seems unsuitable for wavelength tuning of the vortex beams for such E‖*c* polarization due to the high threshold pump power and serious thermal lens effects.

Next, we studied the wavelength tuning performance of the vortex laser for E‖*b* polarization by rotating the laser crystal. Figure 4(a) shows the output power with respect to the absorbed pump power. Without the BF, the threshold absorbed pump powers were 2.73 W and 2.57 W for the $LG_{0,+1}$ and $LG_{0,-1}$ modes, corresponding to the slope efficiencies of 25% and 27.1%, respectively. The inset shows their optical spectra with the peak wavelength located at 1950.9 nm and 1953.8 nm,

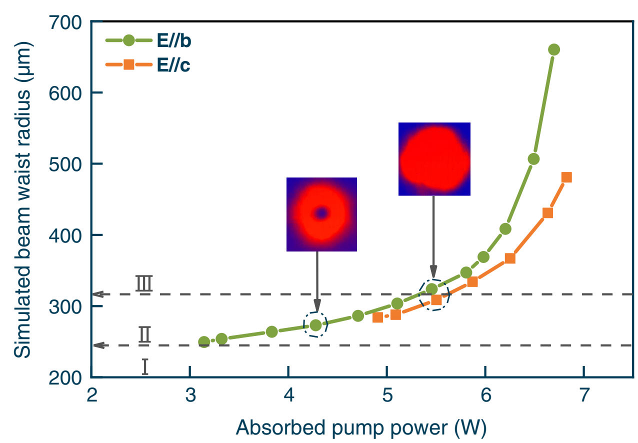

Fig. 3. Simulated beam radius of laser in the YAP crystal as a function of absorbed pump power by considering the thermal lens effect. Inset: beam profiles of the output laser at different pump powers.

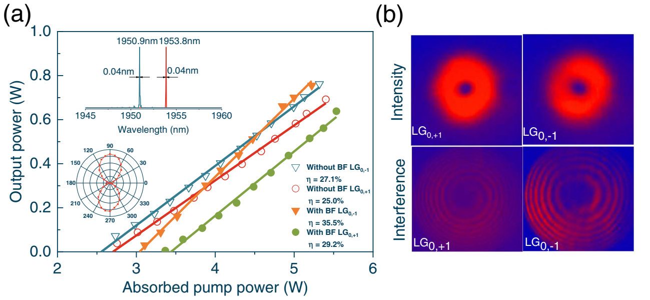

Fig. 4. (a) Laser output performance of the $LG_{0,+1}$ modes with and without the BF. (b) Beam profiles and the corresponding interference fringe patterns of $LG_{0,+1}$ and $LG_{0,-1}$ modes. Insets in (a): optical spectra and polarization measurement of $LG_{0,+1}$ and $LG_{0,-1}$ modes without the BF in the cavity.

respectively. Similarly, the vortex laser was linearly polarized along the *b*-axis direction owing to the natural birefringence. By inserting the BF into the laser cavity, wavelength tuning of $LG_{0,+1}$ and $LG_{0,-1}$ modes was, respectively, realized. To confirm the OAM of the produced optical vortices, we measured the beam profiles and the corresponding self-interference fringe patterns by using a CCD camera and a homemade Mach–Zehnder interferometer. As shown in Fig. 4(b), a clean doughnut-beam profile without other obvious transverse modes and the clear interference fringes indicate the high purity of the generated $LG_{0,+1}$ (or $LG_{0,-1}$) mode.

For the $LG_{0,+1}$ mode, the maximum output power was 0.64 W with a slope efficiency of 29.2%, and, in the whole pump power range, the optical vortex can be well maintained. As shown in Fig. 5(a), the wavelength was tunable from 1934.9 to 1993.3 nm at an output power of 0.3 W, corresponding to a range of 58 nm.

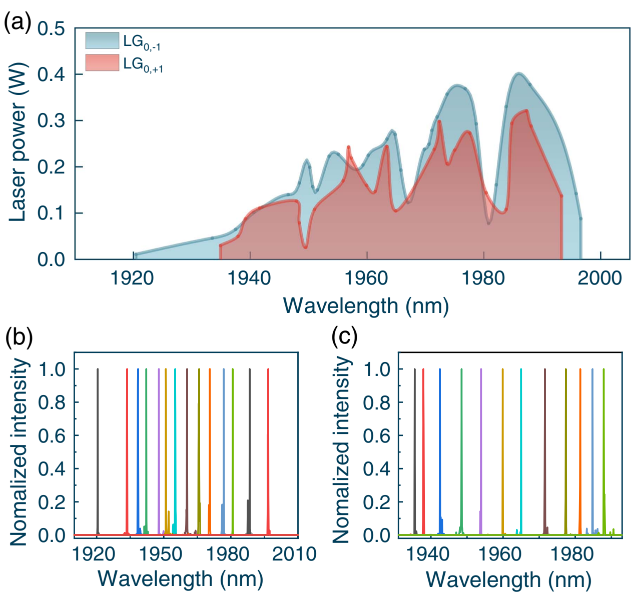

Fig. 5. (a) Measured tuning spectra for $LG_{0,+1}$ and $LG_{0,-1}$ modes at the fixed absorbed pump power of 4.27 W. (b) and (c) The measured spectral lines at several typical wavelengths for the $LG_{0,+1}$ and $LG_{0,-1}$ modes.

Figure 5(b) shows the optical spectra at different emission peaks, the spectral full width at half-maximum (FWHM) in the full range was less than 50 pm, which should be helpful for the high-purity vortex laser operation[28]. In comparison, the $LG_{0,-1}$ mode exhibited a better performance, which may be caused by the lower introduced losses for generation of such a mode. A maximum output power of 0.76 W was achieved with a slope efficiency of 35.5%. The wavelength tuning range was broadened to more than 76 nm, from 1920.4 to 1996.6 nm. It should be emphasized that a wider tuning range from 1913.4 to 2008.4 nm could be obtained in this case; however, the spatial phase front has been destroyed, leading to beam distortion at the extended spectral region. Nevertheless, the range achieved in the present work is much broader than the previous reports based on the VBG or BF operating in the near-IR region[20,30–34].

4. Conclusion

In summary, we reported on the first, to the best of our knowledge, wavelength-tunable vortex laser in the 2 μm spectral range by employing a BF. A continuous tuning range of 76 nm from 1920.4 to 1996.6 nm has been demonstrated for the $LG_{0,-1}$ mode, with a typical linewidth of less than 50 pm. In the present work, further power scaling of the vortex laser or a broader wavelength running range was limited by thermally induced beam distortion and mode mixing. Therefore, a cavity design with a large beam waist and optimization of the cooling system will be the next step to improve the laser performances. Nevertheless, this work, as a proof of principle study, shows that the BF can be employed as an effective wavelength selector for the $LG_{0,\pm1}$ mode in the 2 μm spectral range with a well-maintained spiral phase front. Such a tunable vortex laser providing a specific wavelength selection and reliable topological charge conversion should have potential application in the field of high-capacity optical communications with wavelength and OAM-MDM.

Acknowledgement

This work was financially supported by the National Natural Science Foundation of China (Nos. 52032009 and 62075090), Natural Science Foundation of Jiangsu Province (Nos. SBK2019030177 and SBX2021020083), and Postgraduates Innovation Program of Jiangsu Province (No. KYCX21_2619).

References

1. L. Allen, M. W. Beijersbergen, R. J. C. Spreeuw, and J. P. Woerdman, "Orbital angular momentum of light and the transformation of Laguerre-Gaussian laser modes," Phys. Rev. A **45**, 8185 (1992).
2. J. Wang, J. Y. Yang, I. M. Fazal, N. Ahmed, Y. Yan, H. Huang, Y. Ren, Y. Yue, S. Dolinar, and M. Tur, "Terabit free-space data transmission employing orbital angular momentum multiplexing," Nat. Photonics **6**, 488 (2012).
3. D. G. Grier, "A revolution in optical manipulation," Nature **424**, 810 (2003).

4. M. P. J. Lavery, F. C. Speirits, S. M. Barnett, and M. J. Padgett, "Detection of a spinning object using light's orbital angular momentum," Science **341**, 537 (2013).
5. M. W. Beijersbergen, L. Allen, H. van der Veen, and J. P. Woerdman, "Astigmatic laser mode converters and transfer of orbital angular momentum," Opt. Commun. **96**, 123 (1993).
6. M. W. Beijersbergen, R. P. C. Coerwinkel, M. Kristensen, and J. P. Woerdman, "Helical-wavefront laser beams produced with a spiral phase plate," Opt. Commun. **112**, 321 (1994).
7. V. Y. Bazhenov, M. V. Vasnetsov, and M. S. Soskin, "Laser-beams with screw dislocations in their wave-fronts," JETP Lett. **52**, 429 (1990).
8. N. Matsumoto, T. Ando, T. Inoue, Y. Ohtake, N. Fukuchi, and T. Hara, "Generation of high-quality higher-order Laguerre–Gaussian beams using liquid-crystal-on-silicon spatial light modulators," J. Opt. Soc. Am. A **25**, 1642 (2008).
9. D. Lin, J. M. O. Daniel, and W. A. Clarkson, "Controlling the handedness of directly excited Laguerre-Gaussian modes in a solid-state laser," Opt. Lett. **39**, 3903 (2014).
10. D. J. Kim and J. W. Kim, "Direct generation of an optical vortex beam in a single-frequency Nd:YVO_4 laser," Opt. Lett. **40**, 399 (2015).
11. D. Lin and W. A. Clarkson, "Polarization-dependent transverse mode selection in an Yb-doped fiber laser," Opt. Lett. **40**, 498 (2015).
12. J. L. Lu, H. F. Lin, G. Zhang, B. X. Li, L. Z. Zhang, Z. B. Lin, Y. F. Chen, V. Petrov, and W. D. Chen, "Direct generation of an optical vortex beam from a diode-pumped Yb:$MgWO_4$ laser," Laser Phys. Lett. **14**, 085807 (2017).
13. C. Y. Fu and Y. P. Lan, "Dynamics of the Laguerre Gaussian $TEM^*_{0,l}$ mode in a solid-state laser," Phys. Rev. A **63**, 063807 (2001).
14. A. Ito, Y. Kozawa, and S. Sato, "Generation of hollow scalar and vector beams using a spot-defect mirror," J. Opt. Soc. Am. A **27**, 2072 (2010).
15. Y. Chen and Y. Lan, "Dynamics of the Laguerre Gaussian TEM_{01} mode in a solid-state laser," Phys. Rev. A **63**, 063807 (2001).
16. Y. Zhao, Z. Wang, H. Yu, S. Zhang, H. Zhang, X. Xu, J. Xu, X. Xu, and J. Wang, "Direct generation of optical vortex pulses," Appl. Phys. Lett. **101**, 031113 (2012).
17. A. Ishaaya, N. Davidson, and A. Friesem, "Very high-order pure Laguerre-Gaussian mode selection in a passive *Q*-switched Nd:YAG laser," Opt. Express **13**, 4952 (2005).
18. Q. Liu, Y. Zhao, M. Ding, W. Yao, X. Fan, and D. Shen, "Wavelength- and OAM-tunable vortex laser with a reflective volume Bragg grating," Opt. Express **25**, 23312 (2017).
19. L. Zhao, Y. Yuan, L. Tong, F. Cai, W. Zhang, and Y. Cai, "Broadly tunable optical vortex beam in a diode-pumped Yb:CALGO laser," Opt. Laser Technol. **141**, 107134 (2021).
20. R. C. Stoneman and L. Esterowitz, "Efficient 1.94-pm Tm:YALO laser," IEEE J. Sel. Top Quantum Electron. **1**, 78 (1995).
21. I. F. Elder and J. Payne, "Diode-pumped, room-temperature Tm:YAP laser," Appl. Opt. **36**, 8606 (1998).
22. G. Ghosh, "Dispersion-equation coefficients for the refractive index and birefringence of calcite and quartz crystals," Opt. Commun. **163**, 95 (1999).
23. X. L. Wang and J. Q. Yao, "Transmitted and tuning characteristics of birefringent filters," Appl. Opt. **31**, 4505 (1992).
24. N. Zhang, Z. X. Wang, S. D. Liu, W. Jing, H. Huang, Z. X. Huang, K. Z. Tian, Z. Y. Yang, Y. G. Zhao, U. Griebner, V. Petrov, and W. D. Chen, "Watt-level femtosecond Tm-doped "mixed" sesquioxide ceramic laser in-band pumped by a Raman fiber laser at 1627 nm," Opt. Express **30**, 23978 (2022).
25. J. W. Kim and W. A. Clarkson, "Selective generation of Laguerre-Gaussian (LG_{0n}) mode output in a diode-laser pumped Nd:YAG laser," Opt. Commun. **296**, 109 (2013).
26. J. Körner, T. Lühder, J. Reiter, I. Uschmann, H. Marschner, V. Jambunathan, A. Lucianetti, T. Mocek, J. Hein, and M. C. Kaluza, "Spectroscopic investigations of thulium doped YAG and YAP crystals between 77 K and 300 K for short-wavelength infrared lasers," J. Lumin. **202**, 427 (2018).
27. Y. Chen, M. M. Ding, J. L. Wang, L. Wang, Q. Y. Liu, Y. G. Zhao, Y. Liu, D. Shen, Z. P. Wang, X. G. Xu, and V. Petrov, "High-energy 2 μm pulsed vortex beam excitation from a *Q*-switched Tm:LuYAG laser," Opt. Lett. **45**, 722 (2020).
28. M. M. Ding, Y. Chen, J. Wang, D. L. Yin, Y. Wang, P. Liu, Y. G. Zhao, D. Y. Tang, D. Y. Shen, Y. Liu, Z. P. Wang, X. G. Xu, and V. Petrov, "2.7 μm optical vortex beam directly generated from an Er:Y_2O_3 ceramic laser," Opt. Lett. **44**, 4973 (2019).
29. D. Lin and W. A. Clarkson, "End-pumped Nd:YVO_4 laser with reduced thermal lensing via the use of a ring-shaped pump beam," Opt. Lett. **42**, 2910 (2017).
30. W. D. Zhang, K. Y. Wei, L. G. Huang, D. Mao, B. Q. Jiang, F. Gao, G. Q. Zhang, T. Mei, and J. L. Zhao, "Optical vortex generation with wavelength tunability based on an acoustically-induced fiber grating," Opt. Express **24**, 19278 (2016).
31. V. S. Lyubopytov, A. P. Porfirew, S. O. Gurbatov, S. Paul, M. F. Schumann, J. Cesar, M. Malekizandi, M. T. Haidar, M. Wegener, A. Chipouline, and F. Küppers, "Simultaneous wavelength and orbital angular momentum demultiplexing using tunable MEMS-based Fabry-Perot filter," Opt. Express **25**, 9634 (2017).
32. Q. Y. Liu, Y. G. Zhao, M. M. Ding, W. C. Yao, and D. Y. Shen, "Wavelength-and OAM-tunable vortex laser with a reflective volume Bragg grating," Opt. Express **25**, 23312 (2017).
33. S. Yao, G. Ren, Y. Shen, Y. Jiang, and S. Jian, "Tunable orbital angular momentum generation using all-fiber fused coupler," IEEE Photon. Technol. Lett. **30**, 99 (2018).
34. M. Gong, F. Xing, and M. Yuan, "Wavelength-tunable Hermite–Gaussian modes and an orbital-angular-momentum-tunable vortex beam in a dual-off-axis pumped Yb:CALGO laser," Opt. Lett. **43**, 291 (2018).